

# Time-dependent quantum harmonic oscillator: a continuous route from adiabatic to sudden changes

D. Martínez-Tibaduiza\*

*Instituto de Física, Universidade Federal Fluminense,  
Avenida Litorânea, 24210-346 Niterói, RJ, Brazil*

L. Pires and C. Farina

*Instituto de Física, Universidade Federal do Rio de Janeiro,  
21941-972 Rio de Janeiro, RJ, Brazil*

In this work we answer the question: how sudden or adiabatic is a change in the frequency of a quantum harmonic oscillator (HO)? To do this, we study a frequency transition with a continuous parameter enabling to tune the speed of the transition from the sudden to the adiabatic limit. We assume the HO is in its fundamental state in the remote past and compute numerically the time evolution operator by employing an iterative method. The resulting state of the system is a vacuum squeezed state, presented in two different bases related by Bogoliubov transformations, of which we fully characterize and discuss squeezing and adiabaticity along the frequency transition. Finally, we obtain analytical approximate expressions relating squeezing with the transition speed as well as the initial and final frequencies. We think our results may shed some light on subtleties and common inaccuracies in the literature related to the adiabatic theorem interpretation for this system.

## I. INTRODUCTION

The harmonic oscillator (HO) is undoubtedly one of the most important systems in physics since it can be used to model a great variety of physical situations both in classical and quantum regimes. In the former case, almost all movements of physical systems with small amplitude around a stable equilibrium configuration are described by harmonic motions which explain, among many other things, why the classical theory of dispersion in dielectrics works so well [1, 2]. In the quantum regime, we can mention many examples, from quantum optics, where for many purposes the quantized modes of the electromagnetic field behave like quantum HOs [3], to quantum chemistry, where the main characteristics of the London-van der Waals forces can be understood by considering two atoms as fluctuating dipoles modeled by oscillating charges interacting through their instantaneous dipole fields [4].

A more general system may be a time-dependent harmonic oscillator (TDHO), *i.e.*, a HO whose parameters: mass, frequency or both, are time-dependent. The TDHO is a very rich system and a natural scenario to study the important squeezed states, appearing in a variety of branches of physics such as quantum optics [5–13], gravitational interferometry [14–21], cosmology [22–27], metrology [28, 29], telecommunications [30], analogue models to the dynamical Casimir effect [31–38] and spin states [39–41], relevant in optical clocks [42]. The main property of these states is to reduce the value of one of the quadrature variances in relation to coherent states, which already saturate the Heisenberg relation [43–45]. This property is known as squeezing.

In one sense, it is well-known that any non-adiabatic change in the parameters of a HO, initially in a coherent state, generates squeezing [46, 47]. On the other hand, adiabatic changes do not produce squeezing and, in this realm, the so-called quantum adiabatic invariants of the system can be identified [31, 46, 48–51]. Nevertheless, realistic changes in the parameters cannot be carried out totally adiabatic as this would imply infinite time. As an important case, the most non-adiabatic change *i.e.*, a sudden change (or, simply a jump) in the frequency of a HO, has exact solution and it has been very well studied and characterized [52–61]. However, up to the authors' knowledge, in the literature there is not a full characterization of squeezing for a continuous interpolation between a sudden and an adiabatic transition, enabling one to answer how sudden or adiabatic is a given change in the parameters of a HO.

In this paper, our purpose is to develop such characterization by studying numerically the evolution of a HO when its frequency presents a transition modelled by a monotonic functions that asymptotically approaches to constant values. These functions contain a continuous parameter that enables one to modify how fast the transition occurs. This kind of time-dependence in frequency enables to avoid possible numerical divergences [36], while the values of the continuous parameter, besides to characterize the sudden and adiabatic limits [47], enables a continuous interpolation between them. The initial state is considered as the fundamental, so the system evolves to a vacuum squeezed state. Using an iterative method developed in Ref. [62] we calculate the state of the system, initially, in the basis that diagonalizes the hamiltonian at  $t = 0$ . Then, in order to identify and clarify some subtleties and usual inaccuracies in the literature, we also describe the system in the basis that diagonalizes the hamiltonian at any time. The aforementioned

---

\* Correspondence to: danielmartinez@gmail.com

bases are related by Bogoliubov transformations and we do explicit calculations for the basis transformation using new BCH-like relations [63]. We discuss squeezing and adiabaticity relative to each basis and to different quadrature operators. This is how we identify the instantaneous quadrature operator as the one time-connected to what we should expect from a measurement, providing a more intuitive interpretation of experimental procedures involving adiabaticity. Finally, we present the continuous interpolation between the sudden and adiabatic transitions. Using numerical analysis we found analytical approximate formulas that enables one to fit the SP as well as the variance of the instantaneous quadrature operator for any transition speed and different values of  $\omega_0$  and  $\omega_f$ , provided they do not differ by a factor greater than 10. The analysis of these results reveals a relevant difference in the squeezing production between enhance or diminish in a non-sudden way the frequency of an HO.

This paper is organized as follows. In Section II we present the mathematical survey for the time evolution of the system. In Section III we perform numerical calculations to analyze squeezing and adiabaticity in a frequency transition. In Section IV we present the continuous interpolation between sudden and adiabatic transitions. Section V is left for the conclusions and final remarks.

## II. TIME EVOLUTION

Consider a one-dimensional HO of unit mass with arbitrary time-dependent frequency,  $\omega(t)$ . Its hamiltonian is given by

$$\hat{H}(t) = \frac{1}{2}\hat{p}^2 + \frac{1}{2}\omega^2(t)\hat{q}^2, \quad (1)$$

where  $\hat{p}$  and  $\hat{q}$  are the usual momentum and position operators in the Schrödinger picture. Let us call  $\hat{H}(t)$  as the *instantaneous* hamiltonian, since it depends explicitly of time. Following Rhodes [53], in order to diagonalize  $\hat{H}(t)$  we introduce the time-dependent operator (we are using  $\hbar = 1$ )

$$\hat{b}(t) \equiv \sqrt{\frac{\omega(t)}{2}} \left( \hat{q} + i\frac{\hat{p}}{\omega(t)} \right). \quad (2)$$

This operator and its hermitian adjoint satisfy the (equal-time) commutation relation:

$$[\hat{b}(t), \hat{b}^\dagger(t)] = 1. \quad (3)$$

Let us now define the usual annihilation operator, namely

$$\hat{a} \equiv \sqrt{\frac{\omega_0}{2}} \left( \hat{q} + i\frac{\hat{p}}{\omega_0} \right), \quad (4)$$

where  $\omega_0 \equiv \omega(t=0)$  and is satisfied  $[\hat{a}, \hat{a}^\dagger] = 1$ . consequently,  $\hat{a}^\dagger$  is the creation operator. Notice that  $\hat{a}$  and  $\hat{a}^\dagger$  coincide with  $\hat{b}(t)$  and  $\hat{b}^\dagger(t)$  at  $t = 0$ , respectively, and

they are used to diagonalize the hamiltonian at  $t = 0$ , namely,  $\hat{H}_0 \equiv \hat{H}(t = 0)$ , as follows

$$\hat{H}_0 |n\rangle = \omega_0 \left( \hat{n} + \frac{1}{2} \right) |n\rangle = \omega_0 \left( n + \frac{1}{2} \right) |n\rangle, \quad (5)$$

with  $\hat{n} = \hat{a}^\dagger \hat{a}$  the number operator,  $|n\rangle = \frac{(\hat{a}^\dagger)^n}{\sqrt{n!}} |0\rangle$ , and, consequently,  $\{|n\rangle\}$  is the Fock space at  $t = 0$ . Let us refer to  $\hat{H}_0$  as the *initial* hamiltonian,  $\{|n\rangle\}$  as the initial basis and operators  $\hat{a}$  and  $\hat{a}^\dagger$  as the initial representation. Using Eqs. (4) to write position and momentum operators in the initial representation, and then replacing them in Eq. (2), we get

$$\hat{b}(t) = \cosh(\rho(t))\hat{a} + \sinh(\rho(t))\hat{a}^\dagger, \quad (6)$$

where

$$\rho(t) \equiv \frac{1}{2} \ln \left( \frac{\omega(t)}{\omega_0} \right). \quad (7)$$

From Eqs. (3) and (6), operators  $\hat{b}(t)$  and  $\hat{b}^\dagger(t)$  are identified as real Bogoliubov transformations of operators  $\hat{a}$  and  $\hat{a}^\dagger$ . In terms of the above operators, the instantaneous hamiltonian, Eq.(1), reads

$$\hat{H}(t) = \omega(t) \left[ \hat{b}^\dagger(t)\hat{b}(t) + \frac{1}{2} \right], \quad (8)$$

therefore, it is diagonal. Since operators  $\hat{b}(t)$  and  $\hat{b}^\dagger(t)$  serve to diagonalize the instantaneous hamiltonian, let us refer to them as the instantaneous representation.

At this time it is convenient to introduce the so-called vacuum squeezed states (for an introduction on squeezed states we suggest Ref. [64]). A single-mode vacuum squeezed state  $|z\rangle$  (referred to, henceforth, simply by squeezed state) of the initial hamiltonian  $\hat{H}_0$ , can be obtained by the application of the squeezing operator,  $\hat{S}(z)$ , on the fundamental state of  $\hat{H}_0$ , namely,  $|z\rangle = \hat{S}(z)|0\rangle$ , with

$$\hat{S}(z) \equiv \exp \left\{ -\frac{z}{2} \hat{a}^{\dagger 2} + \frac{z^*}{2} \hat{a}^2 \right\}, \quad (9)$$

where  $z = re^{i\varphi}$  is a complex number and  $*$  indicates complex conjugation. Notice that  $z$ , and hence parameters  $r$  and  $\varphi$ , determines uniquely the squeezed state. To interpret  $r$  and  $\varphi$ , let us introduce the quadrature operator  $\hat{Q}_\lambda$ , defined by [64]

$$\hat{Q}_\lambda = \frac{1}{\sqrt{2}} [e^{i\lambda} \hat{a}^\dagger + e^{-i\lambda} \hat{a}], \quad (10)$$

satisfying the commutation relation  $[\hat{Q}_\lambda, \hat{Q}_{\lambda+\pi/2}] = i$ . It is important to note that, rather than position and momentum operators, the quadrature operator is frequency dependent. In fact, from its definition and Eq. (4), it is related to  $\hat{q}$  and  $\hat{p}$  by fixing the value of  $\lambda$ ,

the quadrature, as  $\hat{Q}_{\lambda=0} = (\hat{a}^\dagger + \hat{a})/\sqrt{2} = \sqrt{\omega_0}\hat{q}$  and  $\hat{Q}_{\lambda=\pi/2} = i(\hat{a}^\dagger - \hat{a})/\sqrt{2} = \hat{p}/\sqrt{\omega_0}$ . The HO is said to be squeezed if the variance of one quadrature is smaller than  $\frac{1}{2}$ , the so-called *coherent limit*. It can be shown that the variance of  $\hat{Q}_\lambda$  in a squeezed state  $|z\rangle$ , is given by [64]

$$(\Delta Q_\lambda)^2 = \frac{e^{2r}}{2} \sin^2(\lambda - \varphi/2) + \frac{e^{-2r}}{2} \cos^2(\lambda - \varphi/2). \quad (11)$$

Notice the explicit dependence of the variance with  $r$  and  $\varphi$ . Further, from the previous equation we see that

$$\frac{e^{-2r}}{2} \leq (\Delta Q_\lambda)^2 \leq \frac{e^{2r}}{2}, \quad (12)$$

which justifies the interpretation of  $r$  as the squeezing parameter (SP). Parameter  $\varphi$  is referred to as the squeezing phase (Sph).

Coming back to the squeezing operator, it is unitary, and transforms the annihilation operator as [53, 64]

$$\hat{S}(z)\hat{a}\hat{S}(-z) = \cosh(|z|)\hat{a} + \frac{z}{|z|} \sinh(|z|)\hat{a}^\dagger. \quad (13)$$

Comparison of the last equation with Eq. (6), enables us to write  $\hat{b} = \hat{S}(\rho)\hat{a}\hat{S}(-\rho)$ , where we have omitted the temporal dependence in the argument of the operators for simplicity of notation. We shall do that along the text whenever there is not risk of confusion. Notice that, from its definition in Eq. (7),  $\rho(t)$  is real valued. Consequently, the SP in  $\hat{S}(\rho)$  is given by  $|\rho(t)|$ , while the Sph will be zero, for  $\omega(t) > \omega_0$ , or  $\pi$ , for  $\omega(t) < \omega_0$ . Using the above results, Eq. (8) can be written as:

$$\hat{H}(t) = \frac{\omega(t)}{\omega_0} \hat{S}(\rho(t)) \hat{H}_0 \hat{S}(-\rho(t)), \quad (14)$$

Hence, we can say that the unitary transformation carried out by  $\hat{S}(\rho)$ , up to the factor  $\frac{\omega(t)}{\omega_0}$ , has the effect to *update* the initial hamiltonian to the instantaneous one. From the above result and Eq. (5), it follows that

$$\hat{H}(t) \left( \hat{S}(\rho(t)) |n\rangle \right) = \omega(t) \left( n + \frac{1}{2} \right) \left( \hat{S}(\rho(t)) |n\rangle \right). \quad (15)$$

Therefore,  $\hat{S}(\rho(t)) |n\rangle$  is an eigenstate of  $\hat{H}(t)$ . Let us write it as  $|n\rangle_t \equiv \hat{S}(\rho(t)) |n\rangle$ . One direct consequence is that, for instance, the fundamental state in the instantaneous basis is a squeezed state in the initial basis, explicitly,

$$|0\rangle_t = \sqrt{\text{sech}(\rho)} \sum_{n=0}^{\infty} \frac{\sqrt{(2n)!}}{n!} \left[ -\frac{1}{2} \tanh(\rho) \right]^n |2n\rangle. \quad (16)$$

This result will be useful in the next section, when discussing the behavior of the SP in a frequency transition of the HO. If we define  $\hat{n}(t) = \hat{b}^\dagger(t)\hat{b}(t)$  as the instantaneous number operator, then  $|n\rangle_t = \frac{(\hat{b}^\dagger(t))^n}{\sqrt{n!}} |0\rangle_t$ , and

$\{|n\rangle_t\}$  is the Fock space at time  $t$ . Henceforth,  $\{|n\rangle_t\}$  will be refereed as the instantaneous basis. Notice that the initial and instantaneous basis coincide at  $t = 0$  and whenever that  $\omega(t) = \omega_0$ .

At this point, it is convenient to introduce the generators of the  $su(1,1)$  Lie algebra in the following form:

$$\hat{K}_+ := \frac{\hat{a}^{\dagger 2}}{2}, \quad \hat{K}_- := \frac{\hat{a}^2}{2} \quad \text{and} \quad \hat{K}_c := \frac{\hat{a}^\dagger \hat{a} + \hat{a} \hat{a}^\dagger}{4}, \quad (17)$$

satisfying the commutation relations

$$[\hat{K}_+, \hat{K}_-] = -2\hat{K}_c \quad \text{and} \quad [\hat{K}_c, \hat{K}_\pm] = \pm \hat{K}_\pm. \quad (18)$$

Using Eqs. (6) and (17), the hamiltonian of Eq. (8) can be written in the initial representation as

$$\begin{aligned} \hat{H}(t) = & 2\omega(t) \cosh(2\rho(t)) \hat{K}_c + \\ & + \omega(t) \sinh(2\rho(t)) (\hat{K}_+ + \hat{K}_-). \end{aligned} \quad (19)$$

Notice that in the above form of the hamiltonian, all the time-dependence is encoded in the coefficients and not in the operators, as it occurs when using the instantaneous representation Eq. (8).

In the following discussion we shall use the solution given in Ref. [62] for a HO with an arbitrary time-dependent frequency, which is very convenient to do numerical analysis. In this reference the authors considered time splitting in  $N$  intervals of equally small enough size  $\tau = t/N$ , such that the time-dependent frequency  $\omega(t)$  and, consequently, the hamiltonian Eq. (19), can be considered constant in each interval. Using algebraic methods the authors showed that, for a HO initially in its fundamental state, the time evolution operator (TEO) of the system can be written as a squeezing operator of the initial hamiltonian *i.e.*,  $\hat{U}(t, 0) = \hat{S}(z)$ . Consequently, the final state of the system, in the initial basis, is a squeezed state  $|z(t)\rangle = \hat{U}(t, 0)|0\rangle$ , with  $z(t) = r(t)e^{i\varphi(t)}$ . Defining the frequency of an interval  $j$  as  $\omega_j := \omega(j\tau)$  with  $j = 1, 2, \dots, N$ , the complex variable  $z(t)$  that characterizes the final state can be calculated from the following generalized continued fraction [62]:

$$\chi_m = a_m - \frac{b_m}{a_m - \frac{1}{a_{m-1} - \frac{b_{m-1}}{a_{m-1} - \frac{1}{\ddots \cdot a_2 - \frac{b_2}{a_2 - \frac{1}{a_1}}}}}}, \quad (20)$$

where

$$a_j = \frac{-i \sinh(2\rho_j) \sin(\omega_j \tau)}{\cos(\omega_j \tau) + i \cosh(2\rho_j) \sin(\omega_j \tau)}, \quad (21)$$

$$b_j = (\cos(\omega_j \tau) + i \cosh(2\rho_j) \sin(\omega_j \tau))^{-2} \quad (22)$$

and  $\rho_j = \frac{1}{2} \ln \left( \frac{\omega_j}{\omega_0} \right)$ . Expressing  $\chi$  in its polar form,  $\chi = |\chi| e^{i\theta}$ , the state vector of the system  $|z(t)\rangle = |r(t)e^{i\varphi(t)}\rangle$  is obtained by the following identifications

$$r(t) = \tanh^{-1} |\chi_N| \quad \text{and} \quad \varphi(t) = \theta_N \pm \pi, \quad (23)$$

with  $N$  big enough to guarantee convergence in the values of the SP,  $r(t)$ , and the Sph,  $\varphi(t)$ .

Recall that Eq.(23) corresponds to the solution using the eigenstates of  $\hat{H}_0$ . The discussion will continue by describing the system using the eigenstates of  $\hat{H}(t)$ . To do that, we shall write the final state,  $|z(t)\rangle$ , in the instantaneous basis. Using the unitary property of the squeezing operator, the final state can be written as

$$\begin{aligned} |z(t)\rangle &= \hat{S}(z(t))|0\rangle \\ &= \hat{S}(z(t))\hat{S}(-\rho(t))|0\rangle_t. \end{aligned} \quad (24)$$

The solution in this approach depends on rewriting the product of the squeezing operators,  $\hat{S}(z(t))\hat{S}(-\rho(t))$ , in the instantaneous representation. To do this, first note that the Bogoliubov transformation, Eq. (6), can be inverted:

$$\hat{a} = \Gamma_1 \hat{b} - \Gamma_2 \hat{b}^\dagger \quad \text{and} \quad \hat{a}^\dagger = \Gamma_1 \hat{b}^\dagger - \Gamma_2 \hat{b}, \quad (25)$$

where we defined

$$\Gamma_1 = \cosh(\rho(t)) \quad \text{and} \quad \Gamma_2 = \sinh(\rho(t)). \quad (26)$$

Also, note that using the commutation relation, Eq. (3), we can define the generators of the  $su(1,1)$  Lie algebra as:

$$\hat{T}_+ := \frac{\hat{b}^{\dagger 2}}{2}, \quad \hat{T}_- := \frac{\hat{b}^2}{2} \quad \text{and} \quad \hat{T}_c := \frac{\hat{b}^\dagger \hat{b} + \hat{b} \hat{b}^\dagger}{4}, \quad (27)$$

satisfying commutation relations analogous to those of Eq. (18), just replacing  $\hat{K} \rightarrow \hat{T}$ . Using Eqs. (25) and (27) in Eq. (9), we can write

$$\hat{S}(z) = \exp \left\{ \lambda_+ \hat{T}_+ + \lambda_c \hat{T}_c + \lambda_- \hat{T}_- \right\}, \quad (28)$$

where we defined

$$\begin{aligned} \lambda_+ &= (z^* \Gamma_2^2 - z \Gamma_1^2) = -\lambda_-^*, \\ \lambda_c &= 2\Gamma_1\Gamma_2(z - z^*). \end{aligned} \quad (29)$$

In the same way, since  $\rho = \rho^*$ , we obtain

$$\hat{S}(-\rho) = \exp \left\{ \rho \hat{T}_+ - \rho \hat{T}_- \right\}. \quad (30)$$

Although the above operator turns out to be a squeezing operator of the instantaneous hamiltonian  $\hat{H}(t)$ , this is not the case for the resulting one in Eq. (28) due to the presence of the term  $\lambda_c \hat{T}_c$ . However, both operators of Eqs. (28) and (30) can be identified as elements of the  $su(1,1)$  Lie algebra and, therefore, we can use new BCH-like relations [63] to calculate their product as

$$\hat{S}(z) \hat{S}(-\rho) = e^{\alpha \hat{T}_+} e^{\beta \hat{T}_c} e^{\gamma \hat{T}_-}, \quad (31)$$

where

$$\begin{aligned} \alpha &= \Lambda_+ + \frac{\Gamma_2 \Lambda_c}{\Gamma_1 - \Gamma_2 \Lambda_-}, & \beta &= \frac{\Lambda_c}{(\Gamma_1 - \Gamma_2 \Lambda_-)^2} \\ \text{and} \quad \gamma &= \frac{\Gamma_1 \Lambda_- - \Gamma_2}{\Gamma_1 - \Gamma_2 \Lambda_-}, \end{aligned} \quad (32)$$

with

$$\begin{aligned} \Lambda_+ &= \frac{(e^{-i\varphi} \Gamma_2^2 - e^{i\varphi} \Gamma_1^2) \sinh(r)}{\cosh(r) - \Gamma_1 \Gamma_2 (e^{i\varphi} - e^{-i\varphi}) \sinh(r)}, \\ \Lambda_- &= \frac{(e^{-i\varphi} \Gamma_1^2 - e^{i\varphi} \Gamma_2^2) \sinh(r)}{\cosh(r) - \Gamma_1 \Gamma_2 (e^{i\varphi} - e^{-i\varphi}) \sinh(r)}, \\ \Lambda_c &= (\cosh(r) - \Gamma_1 \Gamma_2 (e^{i\varphi} - e^{-i\varphi}) \sinh(r))^{-2}. \end{aligned} \quad (33)$$

Finally, using the following results

$$\begin{aligned} \hat{T}_- |n\rangle_t &= \frac{1}{2} \sqrt{n(n-1)} |n-2\rangle_t, \\ \hat{T}_+ |n\rangle_t &= \frac{1}{2} \sqrt{(n+1)(n+2)} |n+2\rangle_t, \\ \hat{T}_c |n\rangle_t &= \frac{1}{2} \left( n + \frac{1}{2} \right) |n\rangle_t, \end{aligned} \quad (34)$$

and the well known expansion  $e^{\hat{A}} = \sum_{n=0}^{\infty} \frac{1}{n!} \hat{A}^n$  (valid for a general operator  $\hat{A}$ ), substitution of Eq. (31) in Eq. (24) yields

$$|z(t)\rangle = \sqrt{|\beta|^{1/2}} \sum_{n=0}^{\infty} \frac{\sqrt{(2n)!}}{n!} \left[ \frac{1}{2} |\alpha| e^{i\vartheta} \right]^n |2n\rangle_t, \quad (35)$$

where the overall phase was removed by the redefinitions

$$\alpha = |\alpha| e^{i\vartheta} \quad \text{and} \quad \beta = |\beta| e^{i\vartheta}. \quad (36)$$

Since the following relation is satisfied

$$|\alpha|^2 + |\beta|^2 = 1, \quad (37)$$

the state vector of the system in the instantaneous basis can also be identified as a squeezed state, but now of the instantaneous hamiltonian  $\hat{H}(t)$ . Let us call the state vector in this basis as  $|\xi(t)\rangle_t$ , with  $\xi(t) = R(t)e^{i\Phi(t)}$ . Therefore,  $R(t)$  and  $\Phi(t)$  are the corresponding SP and Sph of  $|\xi(t)\rangle_t$  and they can be calculated from the complex variable  $\alpha$  in Eq. (32) as

$$R(t) = \tanh^{-1} |\alpha| \quad \text{and} \quad \Phi(t) = \vartheta \pm \pi. \quad (38)$$

We have shown that the state vector of a HO, initially in its fundamental state and whose frequency begins to change in time, evolves to a squeezed state of the initial basis when the eigenstates of the initial hamiltonian are used as the basis. Further, when the eigenstates of the instantaneous hamiltonian are used as the basis, the state vector of the HO also evolves to a squeezed state but of the instantaneous basis. In the next section, considering a transition in the frequency of the HO, we compare the time evolution of the SP's related to both bases.

### III. SQUEEZING AND ADIABATICITY IN A FREQUENCY TRANSITION

In this section we discuss squeezing in a frequency transition of the HO and how it is related to adiabaticity. Let

us consider the following family of hyperbolic tangent functions [36]:

$$\omega(t) = \frac{\omega_f + \omega_0}{2} + \frac{(\omega_f - \omega_0)}{2} \tanh\left(\frac{t - t_0}{\epsilon}\right), \quad (39)$$

where  $\omega_0$  and  $\omega_f$  are the HO frequencies achieved asymptotically in the limits of remote past ( $t \rightarrow -\infty$ ) and distant future ( $t \rightarrow +\infty$ ), respectively,  $t_0$  is the instant for which the HO frequency assumes the average value between  $\omega_0$  and  $\omega_f$  and  $\epsilon$  is, by assumption, a non-negative continuous parameter, with dimensions of time, that can be adjusted appropriately for our purposes. This parameter controls how sudden or slow is the transition from  $\omega_0$  to  $\omega_f$ , and the smaller  $\epsilon$  is the faster the transition will be. In fact, from Eq. (39) it can be shown that

$$\epsilon = \frac{\omega_f - \omega_0}{\omega_f + \omega_0} \left( \frac{\omega(t)}{\dot{\omega}(t)} \right) \Big|_{t=t_0}, \quad (40)$$

where the overdot indicates derivative taken with respect to time. The limiting case  $\epsilon \rightarrow 0$  corresponds to a sudden change at  $t = t_0$ , and the case  $\epsilon \rightarrow \infty$  corresponds to a totally smooth change. Parameter  $\epsilon$  also allows us to define the *transition interval*, denoted by  $\mathcal{I}$ , as the time interval (around  $t_0$ ) in which the frequency changes appreciably. Due to the features of the hyperbolic function and the set of parameters we shall use in the following sections, we choose  $\mathcal{I} \equiv (t_0 - 3\epsilon, t_0 + 3\epsilon)$ . Without any loss of generality, let us set for numerical calculations  $\omega_0 = 1$ ,  $\omega_f = 3$  and  $t_0 = 10$  (in arbitrary units). Consequently, although the HO frequency coincides with  $\omega_0$  only in the remote past, we will consider that, for  $t < t_0 - 3\epsilon$ ,  $\omega(t)$  can be safely approximated by  $\omega_0$ . Therefore, the state vector of the HO can be considered as being its fundamental state for  $t < t_0 - 3\epsilon$ . Similarly, we assume that  $\omega(t)$  has already achieved its asymptotic value  $\omega_f$  for  $t > t_0 + 3\epsilon$ . In panel (a) of Fig. 1 we plot the frequency given by Eq. (39) as a function of time for different values of  $\epsilon$ , namely,  $\epsilon = 10^{-3}, 0.5, 1.0$  and  $1.5$ . Clearly, from this graphic  $\epsilon = 10^{-3} \sim 0$  corresponds to the fastest transition while  $\epsilon = 1.5$  corresponds to the slowest one. As we shall see, the previous choices for  $t_0$  and  $\epsilon$  will be quite good for our discussion.

### A. Squeezing parameter and the adiabatic theorem

As we have shown in Section II, the same state vector of the HO with a time-dependent frequency can be written in two different, but equivalent ways, namely: as a squeezed state relative to the initial hamiltonian,  $|r(t)e^{i\phi(t)}\rangle$ , or as a squeezed state relative to the instantaneous hamiltonian,  $|R(t)e^{i\Phi(t)}\rangle$ . Our purpose here is to analyze the time evolution of the SP's  $r(t)$  and  $R(t)$ , under the light of the adiabatic theorem, assuming that the time-dependent frequency is given by Eq.(39).

### 1. SP in the initial basis

Using Eqs. (20)-(23), we calculate the SP of the HO at a generic instant  $t > 0$  in the initial basis  $\{|n\rangle\}$ , namely,  $r(t)$ . We plot  $r(t)$  as a function of time in Fig. 1(b) employing the same values for  $\epsilon$  as those used in Fig. 1(a). From this figure it can be noted that, once the transition has occurred ( $t > t_0 + 3\epsilon$ ),  $r(t)$  acquires a periodic behavior. The faster the transition is (the smaller  $\epsilon$  is), the earlier the periodic behavior is achieved. Also, for  $t > t_0 + 3\epsilon$  both, the period and the mean value of  $r(t)$ , are the same for all transitions. With this fact in mind, and recalling that the case of a sudden change in the frequency ( $\epsilon = 0$ ) has analytic solution, let us infer some relevant characteristics of all the transitions from this particular limiting case. For a sudden change (jump) in the frequency the SP can be written as [61]

$$r_{\epsilon=0}(t) = \text{arcosh} \sqrt{1 + \left( \frac{\omega_f^2 - \omega_0^2}{2\omega_0\omega_f} \right)^2 \sin^2(\omega_f t)}. \quad (41)$$

A direct inspection of the above equation shows that the period of  $r_{\epsilon=0}(t)$  is  $T = \pi/\omega_f$ , since  $r_{\epsilon=0}(t + \pi/\omega_f) = r_{\epsilon=0}(t)$ . Therefore, the period of  $r(t)$  for any transition is also  $T$ . Now, from Eq. (41) it can be shown that the (periodic) maximum of  $r_{\epsilon=0}(t)$  is  $2\rho_f$  (upper horizontal line) with  $\rho_f = \frac{1}{2} \ln \left( \frac{\omega_f}{\omega_0} \right) = \rho(t > t_0 + 3\epsilon)$  (see Eq. (7)), while the (periodic) minimum of  $r_{\epsilon=0}(t)$  is zero. Hence, once the transition has occurred, for any transition speed (any value of  $\epsilon$ ) the mean value of  $r(t)$  is  $\rho_f$  (lower horizontal line). Finally, it can be noted from Fig. 1(b) that, the slower the transition, the smaller the amplitude of  $r(t)$  and the smoother the oscillations. This enables us to conclude that the period and the average value of the oscillations depend only on the initial and final frequency values, while the amplitude of oscillations is a signature of the speed of the frequency transition.

The behavior of the amplitude can be understood under the light of the adiabatic theorem. Essentially, this theorem states that, along an adiabatic transition, the instantaneous state of the system remains the same [65]. In the present case this means that the state of the system should approximate the fundamental state of  $\hat{H}(t)$  as the transition becomes slower. Recall that the fundamental state of  $\hat{H}(t)$  in the instantaneous basis is a squeezed state in the initial basis, namely,  $|0\rangle_t = \hat{S}(\rho(t))|0\rangle = |\rho(t)\rangle$  (see Eq. (16)). Hence, when the system approaches the adiabatic limit, the state vector in the initial basis must satisfy  $|r(t)e^{i\varphi(t)}\rangle \rightarrow |\rho(t)\rangle$ . Also, since  $\rho(t)$  can take only positive values because we choose  $\omega(t) > \omega_0$ , then we should have  $r(t) \rightarrow \rho(t)$  and  $\varphi(t) \rightarrow 2n\pi$ , with  $n = 0, 1, 2, 3, \dots$ . And this is exactly what occurs: it can be shown that, for any value of  $\epsilon$ , once the transition has occurred the mid-range of  $r(t)$  follows  $\rho(t)$ . Consequently, the decreasing in the amplitude of the oscillations for larger values of  $\epsilon$  guarantees that  $r(t)$  will be closer to  $\rho(t)$  as the transition becomes slower. In fact,

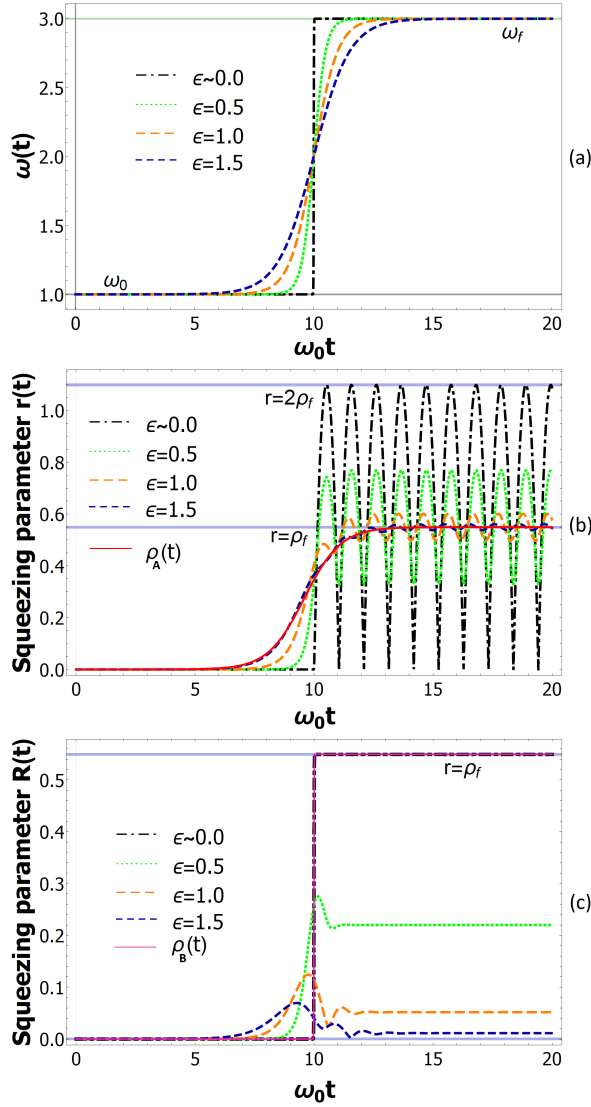


FIG. 1. (a) HO frequency given by Eq. (39) as a function of time; (b) time evolution of the SP in the initial hamiltonian representation and (c) time evolution of the SP in the instantaneous hamiltonian representation. In all panels, different line patterns mean different values of  $\epsilon$ ;  $\epsilon \sim 0.0$  (dot-dashed line and sudden limit),  $\epsilon = 0.5$  (dotted line),  $\epsilon = 1.0$  (long dashed line) and  $\epsilon = 1.5$  (short dashed line and adiabatic limit). The solid lines  $\rho_A(t)$  (in panel (b)) and  $\rho_B(t)$  (in panel (c)) are the plots of  $\rho(t)$  (Eq. (7)) as a function of  $\omega_0 t$  with  $\omega(t)$  given by  $\epsilon = 1.5$  and  $\epsilon \sim 0.0$ , respectively.

as it can be appreciated in Fig. 1(b), for  $\epsilon = 1.5$  (short dashed line)  $r(t)$  is almost totally superposed to  $\rho_A(t)$  (solid line), the latter being  $\rho(t)$  with  $\omega(t)$  evaluated for the same  $\epsilon$ . Although this description is consistent with the adiabatic theorem, it may seem a little bit counterintuitive the fact that the SP has a non zero value in this case. However, this is a direct consequence of the basis chosen for describing the state of the system and, as we shall see in the following subsection, had we employed the instantaneous basis the SP would be zero after the transition (in the adiabatic limit).

## 2. SP in the instantaneous basis

To highlight important connections of the SP to observables and get a more intuitive interpretation of the adiabatic theorem, we shall now describe the SP of the state vector in the instantaneous basis, namely,  $R(t)$ . Using Eqs. (26), (32), (33) and (38), we calculate  $R(t)$  for the frequency of Eq. (39). Its behavior as a function of time is presented in Fig. 1(c), with the same values for  $\epsilon$  as before. As it can be seen in this figure, in contrast to what happens with  $r(t)$ , after the transition has occurred  $R(t)$  has a constant behavior, instead to a periodic one. Interestingly, for a frequency jump the state vector of the system seems to suffer a discontinuity in its magnitude at  $t = t_0$ . However, this is not the case, since as pointed out by Janszky in Ref. [59], even in such a case the TEO satisfy  $\lim_{t \rightarrow t_0} \hat{U}_{\epsilon \rightarrow 0}(t, t_0) = 1$ . Another interesting fact in this description is that  $R(t)$  approaches  $\rho(t)$  in the sudden case, and not in the adiabatic one as it occurs for  $r(t)$ . In fact, as it can be noted in Fig. 1(c), for  $\epsilon \sim 0$  (dot-dashed line and sudden limit),  $R(t)$  and  $\rho_B(t)$  are almost superposed, the latter being  $\rho(t)$  with  $\omega(t)$  evaluated at the smallest value of  $\epsilon$ . Consequently, the maximum value reached by  $R(t)$  is  $\rho_f$ , occurring for a jump in the frequency. Finally, in this basis the adiabatic theorem indicates that  $R(t)$  should approach to zero as the transition becomes slower, since  $|\xi(t)\rangle_t \rightarrow |0\rangle_t$  as  $\epsilon \rightarrow \infty$ . This behavior is evidenced in Fig. 1(c) and, therefore, this basis provides a more direct and intuitive interpretation for the adiabatic theorem. Notice that, regardless of the basis chosen to represent the state, the behavior of the SP provides a simple way to interpret the adiabatic theorem for our system.

## B. Quadrature variances and the adiabatic theorem

As it is well known, observables do not depend on the state basis representation. Accordingly, we can use indifferently  $|z(t)\rangle$  or  $|\xi(t)\rangle_t$  for the variance calculations. However, as we shall show, depending on the selected basis, we can gain some insights about observables interpretation, as well as get some simplifications in the calculations.

Let us begin by analyzing the variance of the quadrature operator  $\hat{Q}_\lambda$  given in Eq. (10), namely,  $(\Delta Q_\lambda)^2$ . Since  $\hat{Q}_\lambda$  is written in terms of annihilation and creation operators  $\hat{a}$  and  $\hat{a}^\dagger$ , it is convenient for calculations to use the state vector in the initial basis,  $|z(t)\rangle$ . Then,  $(\Delta Q_\lambda)^2$  is given by Eq. (11), with  $r$  and  $\varphi$  given by Eqs. (23). In Fig. 2(a) this variance is plotted as a function of time for the squeezed quadrature  $(\Delta Q)^2 \equiv (\Delta Q_{\lambda=0})^2$ , and some similarities with Fig. 1(b) are evident. The most relevant one is that  $(\Delta Q)^2$  is an oscillating function with the same period  $T = \pi/\omega_f$  as  $r(t)$ . The coherent limit, given by  $\sigma_{coh} = 1/2$ , is the maximum possible value for  $(\Delta Q)^2$ , and it can only be (periodically) reached in the

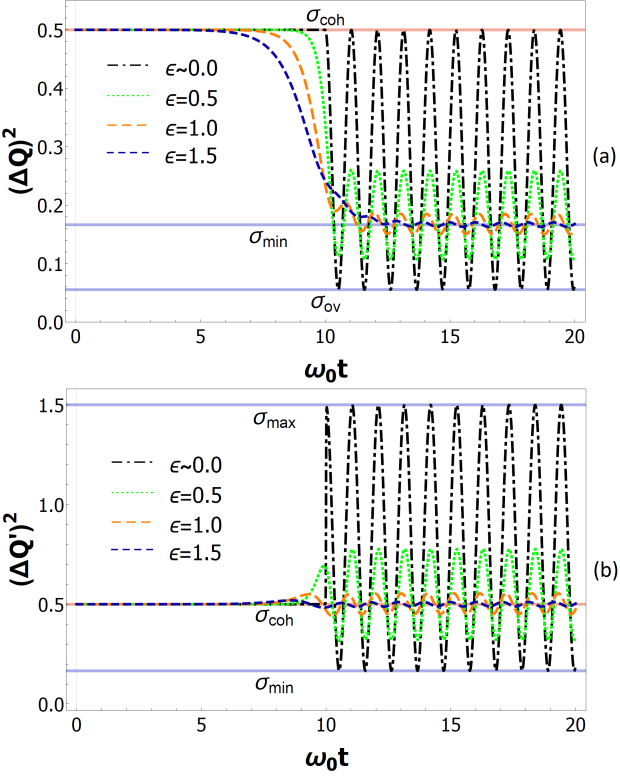


FIG. 2. Variances of (a) the quadrature operator given in Eq. (10), and (b) the instantaneous quadrature operator of Eq. (42). The curves are associated to the same values of the parameter  $\epsilon$  as in Fig. 1 and the same time-interval.

case of a frequency jump. In such a case it is also reached the minimum possible value for  $(\Delta Q)^2$ , and therefore the maximum squeezing. To find this minimum, we evaluate the lower limit of the variance (see Eq. (12)) in the maximum value of  $r(t)$  achieved with a frequency jump, given by  $r(t) = 2\rho_f$ , obtaining  $\sigma_{ov} = \frac{1}{2}(\frac{\omega_0}{\omega_f})^2$ , plotted as the lower horizontal line in Fig. 2(a). It can also be shown that  $\sigma_{min} = \frac{\omega_0}{2\omega_f}$ , as the result from the evaluation of the lower limit of the variance in the mean value of  $r(t)$  after the transition, namely,  $\rho_f$ , plotted as the middle horizontal line in Fig. 2(a). From this figure it can be noted that, after the transition is completed, the mean value of the oscillations does not have a constant value for all the transitions, but decrease from  $\sigma_{ov}/2$  (sudden limit case), to a value  $\sigma_{min}$  (adiabatic limit). Consequently, looking at the system once the transition occurred, the amplitude of the variance oscillations decreases from the maximum  $\frac{\sigma_{coh} - \sigma_{ov}}{2} = \frac{1}{4} \left(1 - \frac{\omega_0^2}{\omega_f^2}\right)$  (sudden limit), to zero (adiabatic limit).

Adiabaticity is therefore related to the decreasing in the amplitude of the oscillations as well as the approach of the mean value of the oscillations to  $\sigma_{min}$ , *i.e.*,  $(\Delta Q)^2 \rightarrow \sigma_{min}$  in the adiabatic limit. Notice that the previous arguments indicate that, from this perspective, the HO start to be squeezed immediately after its fre-

quency starts to change, and remains squeezed even for an adiabatic transition. Regarding the above, an important comment is in order here. In some works, the adiabatic theorem has been interpreted for this system as the approach of  $(\Delta Q_\lambda)^2$  to the coherent limit  $\sigma_{coh}$ , instead to  $\sigma_{min}$  (see for instance [56, 66]). However, as we have shown, for a frequency transition  $r(t)$  is always bigger than zero, even in the adiabatic transition, and, since  $(\Delta Q_\lambda)^2$  is given by Eq. (11), there will be always a squeezed quadrature.

In addition to the quadrature operator  $\hat{Q}_\lambda$ , let us introduce the instantaneous quadrature operator (see Eq. (14)), given by

$$\hat{Q}'_\lambda(t) = \hat{S}(\rho(t)) \hat{Q}_\lambda \hat{S}(-\rho(t)) = \frac{1}{\sqrt{2}} \left[ e^{i\lambda} \hat{b}^\dagger(t) + e^{-i\lambda} \hat{b}(t) \right]. \quad (42)$$

The above operator is the equivalent to change  $\hat{a} \rightarrow \hat{b}$  and  $\hat{a}^\dagger \rightarrow \hat{b}^\dagger$  in Eq. (10). Let us now calculate the variance of this operator, namely,  $(\Delta Q'_\lambda)^2$ . Since  $\hat{Q}'_\lambda$  is expressed in terms of  $\hat{b}(t)$  and  $\hat{b}^\dagger(t)$ , it is convenient to use the state vector in the instantaneous basis,  $|\xi(t)\rangle_t$ , for the variance calculation. In this manner,  $(\Delta Q'_\lambda)^2$  is given by Eq. (11), but this time with the SP and Sph given by Eqs. (38), namely,

$$(\Delta Q'_\lambda)^2 = \frac{e^{2R}}{2} \sin^2(\lambda - \Phi/2) + \frac{e^{-2R}}{2} \cos^2(\lambda - \Phi/2). \quad (43)$$

This variance is plotted as a function of time in Fig. 2(b) for the same quadrature ( $\lambda = 0$ ), that is,  $(\Delta Q')^2 \equiv (\Delta Q'_{\lambda=0})^2$ . As it can be noted from this figure, the variance starts from the coherent limit and acquires an oscillatory periodic behavior, with period  $T = \pi/\omega_f$ , as soon as the transition is completed. This behavior is independently of the value of  $\epsilon$  and due solely to the squeezing phase dynamics, since after the transition  $R(t)$  remains constant (see Fig. 1(c)). The (periodic) maximum  $\sigma_{max} = 1.5$  and minimum  $\sigma_{min}$  possible values of  $(\Delta Q')^2$  are achieved with a frequency jump, and can be calculated by evaluating the highest and lowest limits of the variance (Eq. (12)) in  $R(t) = \rho_f$ , respectively. Accordingly,  $(\Delta Q')^2$  is not always squeezed, as occurs with  $(\Delta Q)^2$  that is always below the coherent limit, but it is periodically squeezed. Notice that, since  $(\Delta Q)^2$  is always squeezed, then  $(\Delta Q_{\lambda=\pi/2})^2$  is always expanded (always above the coherent limit). Nevertheless, due to the oscillatory behavior of  $(\Delta Q')^2$  around the coherent limit, the other quadrature variance,  $(\Delta Q'_{\lambda=\pi/2})^2$ , has a similar behavior to  $(\Delta Q')^2$  with the same (periodic) maximum and minimum values once the transition has occurred.

Let us recall that, as for  $(\Delta Q)^2$ , adiabaticity in  $(\Delta Q')^2$  is related to the decreasing in the amplitude of the oscillations, but this time, in addition, and as the most remarkable characteristic, in the limit of an adiabatic

transition  $(\Delta Q')^2$  approach the coherent limit  $\sigma_{coh}$ , as expected from the adiabatic theorem. From the above discussion one could say that  $(\Delta Q'_\lambda)^2$  is an observable for which the adiabatic theorem can be naturally interpreted.

#### IV. CONTINUOUS INTERPOLATION: FROM SUDDEN TO ADIABATIC

In this section we discuss how squeezing behaves in the HO when the time-dependent functions that describe the frequency transition from an initial value to a final one interpolates continuously the sudden and the adiabatic limits. More specifically, we shall analyze how the final values of the SP  $R(t)$  and the minimal values of the variance  $(\Delta Q')^2$  (both values achieved after the transition has been completed) vary as  $\epsilon$  interpolates continuously the sudden and adiabatic limits. We use numerical analysis to obtain analytical approximate formulas enabling us to fit these final values of  $R(t)$  and the minimum of  $(\Delta Q')^2$ , as a function of  $\epsilon$  and the initial and final frequencies. As we shall see, our fits are in excellent agreement with the exact (numerical) values when the frequencies are in the same order of magnitude. The choices of  $R(t)$  and  $(\Delta Q')^2$  instead to  $r(t)$  and  $(\Delta Q)^2$  are justified by the discussion of the previous section. Recalling that  $(\Delta Q'_\lambda)^2$  has the same (periodic) maximum and minimum final values for  $\lambda = 0$  or  $\lambda = \pi/2$ , in this section we shall write  $(\Delta Q')^2$  to identify both of them.

Let  $R(t_f; \epsilon)$  be  $R(t)$  evaluated at instants such that  $t > t_0 + 3\epsilon$ , *i.e.*, after the transition has effectively occurred. We start by analysing numerically how  $R(t_f; \epsilon)$  varies as a function of  $\epsilon$  for an initial frequency chosen as  $\omega_0 = 1$  and different final values of the frequency, with  $\omega_f > \omega_0$ . These exact (numerical) results correspond to the pointed pattern of Fig. 3. For instance, the (green) square points in this figure correspond to the case  $\omega_0 = 1$  and  $\omega_f = 3$ , and therefore they show how the final height of the SP, plotted in Fig. 1(c), changes from its largest possible value  $R(t_f; \epsilon = 0) = \rho_f$ , produced by a frequency jump, to its smallest possible one  $R(t_f; \epsilon \rightarrow \infty) = 0$ , obtained for an adiabatic transition. As expected,  $R(t_f; \epsilon)$  presents monotonically decreasing behavior as  $\epsilon$  is increased and, consequently, the faster the frequency transition occurs, the higher the reached value of the SP.

Now, let us do an analogous analysis for the quadrature variances. Let  $(\Delta Q')^2(t_f; \epsilon)$  be the minimal value of  $(\Delta Q')^2$  once the transition has occurred. In the inset of Fig. 3 the pointed patterns show the exact results for  $(\Delta Q')^2(t_f; \epsilon)$  as a function of  $\epsilon$  in the same range of values used in the analysis of  $R(t_f; \epsilon)$ . Moreover, we also consider the same set of initial and final frequencies as before. For instance, the (green) square points in the inset correspond to the case  $\omega_0 = 1$  and  $\omega_f = 3$ , and therefore these points show how the smallest value of  $(\Delta Q')^2$

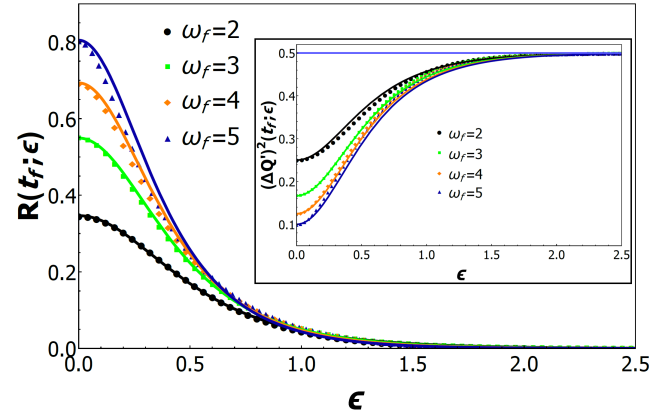


FIG. 3.  $R(t_f; \epsilon)$  as a function of  $\epsilon$  for  $\omega_0 = 1$  and different values of  $\omega_f > \omega_0$ . The pointed patterns are the numerical results and the solid lines correspond to the fitted results using Eq. (44). In the inset is plotted  $(\Delta Q')^2(t_f; \epsilon)$  as a function of  $\epsilon$  for the same values of  $\omega_0$  and  $\omega_f$ . The pointed patterns corresponds to the numerical results while the solid lines correspond to the fitted results using Eq. (45).

(achieved after the frequency transition has occurred, see Fig. 2(b)) changes from  $(\Delta Q')^2(t_f; \epsilon = 0) = \sigma_{min}$ , produced by a frequency jump, to  $(\Delta Q')^2(t_f; \epsilon \rightarrow \infty) = \sigma_{coh}$ , obtained in an adiabatic transition.  $(\Delta Q')^2(t_f; \epsilon)$  presents, as expected, monotonic behavior as we change  $\epsilon$ , and the inset plots resemble those obtained for  $R(t_f; \epsilon)$ , after performing a reflection and a translation.

A comment is in order here: up to the authors knowledge, there is not an analytical expression that enables one to calculate exactly the correspondent SP for an arbitrary time-dependent frequency of the HO. Hence, some efforts have been made to accomplish this task. For instance, a successful approximate analytical expression that works well in the sudden limit as well as in the adiabatic one was obtained in the context of analogue models [36, 67]. However, for the same frequency modulation as in Eq. (39), for transitions characterized by values of  $\epsilon$  between the above two limits (sudden and adiabatic), this formula does not lead to a monotonically decreasing behavior and, consequently, it is no longer valid in this intermediate regime, as correctly stated by these authors. It is therefore natural to look for an analytical expression for  $R(t_f; \epsilon)$  as a function of the initial and final frequencies, in addition to  $\epsilon$ . Recalling that  $\rho_f = \frac{1}{2} \ln \left( \frac{\omega_f}{\omega_0} \right) = \rho(t > t_0 + 3\epsilon)$ , we used numerical analysis to obtain the following analytical approximate expression

$$R(t_f; \epsilon) = |\rho_f| \operatorname{sech} (2 [|\rho_f| + 1] \omega_{min} \epsilon), \quad (44)$$

where  $\omega_{min} = \min \{\omega_0, \omega_f\}$ , providing extremely good fittings for  $R(t_f; \epsilon)$ . For instance, for the choice made previously, namely,  $\omega_0 = 1$  and  $\omega_f = 3\omega_0$ , we should set  $\omega_{min} = \omega_0$  in Eq. (44) to calculate the corresponding fitting. In Fig. 3 we plot with solid lines  $R(t_f; \epsilon)$  as

a function of  $\epsilon$  using our fitting given by Eq. (44) for the same set of frequencies used in our numerical results (point patterned plots). As it can be seen in that figure, the fitting works very well for  $\omega_f/\omega_0 \leq 5$  (error smaller than a few percents) and the agreement gets better the closer the initial and final frequencies are.

Now, as we did for  $R(t_f; \epsilon)$ , we used numerical analysis to obtain an analytical approximate expression for  $(\Delta Q')^2(t_f; \epsilon)$ , namely,

$$(\Delta Q')^2(t_f; \epsilon) = \frac{1}{2} + \frac{1}{2} \left( \frac{\omega_{min}}{\omega_{max}} - 1 \right) \times \text{sech} \left( 5 \tanh \left( \frac{\omega_{min}}{2\omega_{max}} \right) \omega_{max} \epsilon \right) \quad (45)$$

where  $\omega_{max} = \max \{\omega_0, \omega_f\}$  i.e., is the largest frequency between the initial and final ones. This expression provides very good fittings for arbitrary initial and final frequencies provided they do not differ by a factor greater than 10. Let us now compare the results of the above formula to our exact numerical results. In the inset of Fig. 3 we plot with solid lines  $(\Delta Q')^2(t_f; \epsilon)$  as a function of  $\epsilon$  using our fitting given by Eq. (45) for the same set of frequencies used in our numerical results (point patterned plots). As it can be seen in that figure, the fitting works very well for  $\omega_{max}/\omega_{min} \leq 5$  (error smaller than a few percents).

Now, using Eq. (44), in Fig. 4 we present contour plots of  $R(t_f; \epsilon)$  as a function of  $\omega_f/\omega_0$  (vertical axis) and  $\omega_0 \epsilon$  (horizontal axis), for the two cases:  $\omega_f/\omega_0 > 1$  (panel (a)) and  $\omega_f/\omega_0 < 1$  (panel (b)). Notice that  $\omega_0$ ,  $\omega_f$  and  $\epsilon$  are free parameters, and the unique restriction is that the frequencies do not differ by a factor greater than 10. These contour plots allow one to explore in a more convenient way the space of parameters of the problem. One can see, for instance, which region of the parameter space will lead to greater values of the SP than another one.

Initially let us consider the case  $\omega_f > \omega_0$ , shown in the contour plot of Fig. 4(a). From this plot, it can be seen, for instance, how  $R(t_f; \epsilon)$  behaves as we vary  $\epsilon$  (with  $\omega_0$  and  $\omega_f$  fixed, since in the horizontal axis we chose the dimensionless parameter  $\omega_0 \epsilon$ ). In other words, we can recover the information contained in Fig. 3. For our choice made previously, namely,  $\omega_0 = 1$  and  $\omega_f = 3\omega_0$ , we can go to Fig. 4(a), draw a straight horizontal line at  $\omega_f/\omega_0 = 3$ , and read the intermediate values of  $R(t_f; \epsilon)$ , given by the contour plot, as we move along this horizontal line from  $\omega_0 \epsilon = 0$  (sudden limit) to the right. It is worth mentioning that, in addition to the choice  $\{\omega_f = 3, \omega_0 = 1\}$ , there are an infinity of other possibilities with the same ratio  $\omega_f/\omega_0 = 3$ . An inspection of Fig. 4(a) also shows that as the ratio  $\omega_f/\omega_0$  tends to 1, the squeezing parameter approaches zero, as expected, since in this case there is no change in the frequency at all.

By the same token, we can also see from this plot how  $R(t_f; \epsilon)$  behaves as we vary the ratio  $\omega_f/\omega_0$  for fixed values of  $\omega_0 \epsilon$ . It suffices to draw now a vertical line and read

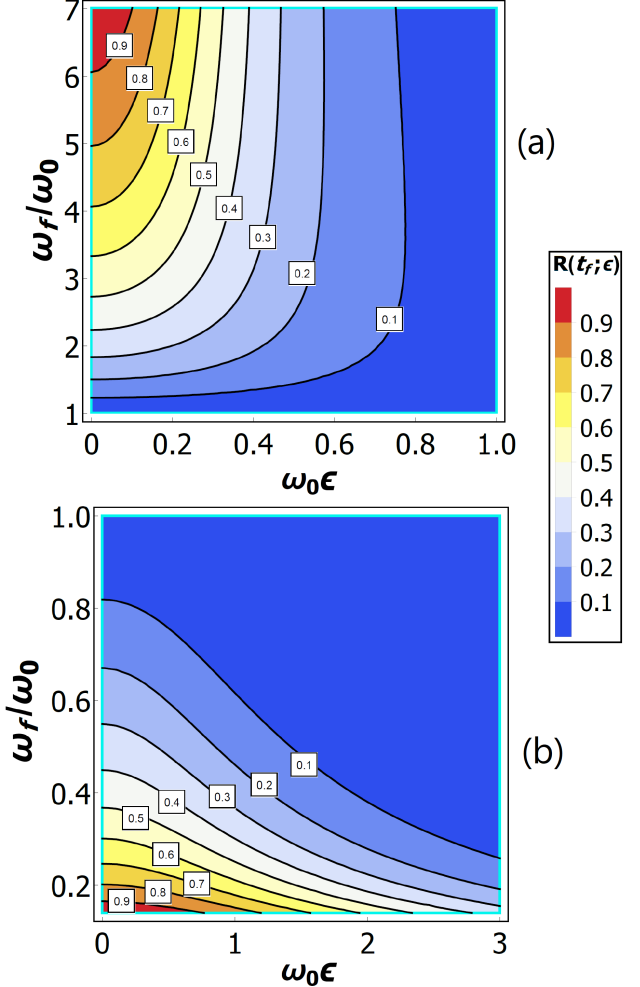


FIG. 4. Contour plots of Eq. (44) for (a)  $\omega_f/\omega_0 > 1$  and (b)  $\omega_f/\omega_0 < 1$ . This graphics enables to relate the squeezing parameter  $R(t_f; \epsilon)$  with relevant parameters of the problem  $\omega_0$ ,  $\omega_f$  and  $\epsilon$ .

the intermediate values of  $R(t_f; \epsilon)$ , given by the contour plot, as we move upwards along this vertical line from the lowest value  $\omega_f/\omega_0 = 1$ . From Fig. 4(a) it is evident that the maximal values achieved by  $R(t_f; \epsilon)$  (top of the vertical lines) becomes smaller as we consider higher values of  $\omega_0 \epsilon$ , as expected, since the greater  $\omega_0 \epsilon$  is the more adiabatic the process will be.

An advantage of the contour plots shown in Fig. 4 is that they provide us with a convenient way to search for the values of the relevant parameters that lead to the desired values of the squeezing parameter. For instance, suppose we want to know the values of  $\omega_f/\omega_0$  and  $\omega_0 \epsilon$  such that  $R(t_f; \epsilon) < 0.1$ . Looking at Fig. 4(a) we see that the answer to this question is the dark blue region in this figure, on the right of the solid black line corresponding to  $R(t_f; \epsilon) = 0.1$ .

For completeness, we show in Fig. 4(b) a contour plot totally analogous to that presented in Fig. 4(a), except for the fact that, now,  $\omega_f < \omega_0$ , so that  $\omega_0$  is the largest

frequency between  $\omega_0$  and  $\omega_f$ . Drawing horizontal and vertical lines, an analysis analogous to the previous one can also be made. As can be checked looking at the contour plots of Fig. 4, for an abrupt change from  $\omega_0$  to  $\omega_f$  (that is, for  $\omega_0\epsilon \rightarrow 0$ ), the value of  $R(t_f; \epsilon)$  will be the same if the ratios  $\omega_f/\omega_0$  and  $\omega_0/\omega_f$  in Fig. 4(a) and Fig. 4(b), respectively, are the same (see the prefactor term in Eq. (44)). However, for finite values of  $\omega_0\epsilon$  this is not true anymore. For instance, take the ratios  $\omega_f/\omega_0 = 5$  in Fig. 4(a) and  $\omega_f/\omega_0 = 0.2$  (which means  $\omega_0/\omega_f = 5$ ) and look at the value  $\omega_0\epsilon = 0.4$ . In the former case, we see that  $0.3 < R(t_f; \epsilon) < 0.4$ , while in the latter case  $0.8 < R(t_f; \epsilon) < 0.9$ . Hence, starting with  $\omega_0$  we will get a larger squeezing if the final frequency is  $\omega_f = \omega_0/5$  instead of  $\omega_f = 5\omega_0$ .

## V. CONCLUSIONS

In this work we considered a harmonic oscillator with a time-dependent frequency described by a function containing a continuous parameter, denoted by  $\epsilon$ , whose values when appropriately chosen can tune from an abrupt change ( $\epsilon \rightarrow 0$ ) to an adiabatic one ( $\epsilon \rightarrow \infty$ ). The main purpose of our work was to compare the time evolution of the squeezing degree of the HO, described by the so called squeezing parameter, for different time evolutions of its frequency (different values of  $\epsilon$ ), from an abrupt change to a totally adiabatic one. In order to enrich our discussion, we did that using two approaches, namely, considering the basis of the instantaneous hamiltonian as well as the basis of the initial hamiltonian. In our discussion it became evident that whenever the final frequency of the HO is different from the initial one, the instantaneous basis is more convenient. Our results are in total agreement with the adiabatic theorem, though there are a few subtleties when the initial basis is used. Then, we tried to answer the question: how sudden or adiabatic is a change in the frequency of a quantum harmonic oscillator (HO)? With this goal, we investigated numerically the behavior of the SP after the change in the frequency was effectively completed, which we denoted by  $R(t_f; \epsilon)$ ,

as a function of parameter  $\epsilon$ . As expected, we showed that  $R(t_f; \epsilon)$  is a monotonically decreasing function of  $\epsilon$ . We used numerical analysis to find analytical expressions that enabled us to obtain quite good fittings for  $R(t_f; \epsilon)$ , as well as for the variance of the instantaneous quadrature operator as functions of the relevant parameters of the problem, namely, parameter  $\epsilon$  and the ratio  $\omega_f/\omega_0$  between the final and initial frequencies (provided this ratio does not exceed one order of magnitude). In order to investigate in a more general way what are the values of the relevant parameters, so that  $R(t_f; \epsilon)$  is restricted to desired intervals, we made some contour plots for  $R(t_f; \epsilon)$  as a function of  $\omega_f/\omega_0$  and  $\epsilon$ . An interesting result that should be emphasized is the following: for an abrupt frequency change, ( $\epsilon \rightarrow 0$ ) the same amount of squeezing will be produced if we enhance or diminish the frequency of the HO by the same proportion. However, for non-sudden transitions (finite values of  $\epsilon$ ), the squeezing degree will be much bigger when the frequency is reduced instead of enhanced by the same ratio.

We think our results can be useful in the construction of more accurate analytical expressions for the SP with other frequency modulations. Also, we expect they may shed some light on subtleties and common inaccuracies in literature related to the interpretation of the adiabatic theorem for this system. Consequently, applications in shortcuts to adiabaticity [68–70], the study of harmonic traps [71–73], characterization of adiabaticity in quantum many-body systems [74] and problems with coupled HO's [75, 76], could be expected.

## VI. ACKNOWLEDGMENTS

The authors acknowledge C. A. D. Zarro, A. L. C. Rego, D. Szilard, Reinaldo F. de Melo e Souza, A. Z. Khouri and P.A. Maia Neto for enlightening discussions. The authors thank the Brazilian agency for scientific and technological research CAPES for partial financial support. This work was partially supported by Conselho Nacional de Desenvolvimento Científico e Tecnológico - CNPq, 310365/2018-0 (C.F.).

---

[1] Andrew Zangwill. *Modern electrodynamics*. Cambridge University Press, 2013.

[2] John David Jackson. *Classical electrodynamics*. John Wiley & Sons, 2007.

[3] Rodney Loudon. *The quantum theory of light*. OUP Oxford, 2000.

[4] Peter W Milonni. *The quantum vacuum: an introduction to quantum electrodynamics*. Academic press, 2013.

[5] Daniel F Walls. Squeezed states of light. *nature*, 306(5939):141, 1983.

[6] Rodney Loudon and Peter L Knight. Squeezed light. *Journal of modern optics*, 34(6-7):709, 1987.

[7] Ling-An Wu, Min Xiao, and H J Kimble. Squeezed states of light from an optical parametric oscillator. *JOSA B*, 4(10):1465, 1987.

[8] Malvin C Teich and Bahaa E A Saleh. Squeezed state of light. *Quantum Optics: Journal of the European Optical Society Part B*, 1(2):153, 1989.

[9] Roy J Glauber and M Lewenstein. Quantum optics of dielectric media. *Physical Review A*, 43(1):467, 1991.

[10] Jan Perina. *Quantum statistics of linear and nonlinear optical phenomena*. Springer Science & Business Media, 1991.

[11] V V Dodonov. Nonclassical states in quantum optics: asqueezed' review of the first 75 years. *Journal of Optics*

*B: Quantum and Semiclassical Optics*, 4(1):R1, 2002.

[12] Victor V Dodonov and Vladimir Ivanovich Man'ko. *Theory of nonclassical states of light*. CRC Press, 2003.

[13] Roman Schnabel. Squeezed states of light and their applications in laser interferometers. *Physics Reports*, 684:1, 2017.

[14] L P Grishchuk and M V Sazhin. Squeezed quantum states of a harmonic oscillator in the problem of gravitational-wave detection. *Soviet Physics-JETP*, 57(6):1128, 1983.

[15] J Gea-Banacloche and G Leuchs. Squeezed states for interferometric gravitational-wave detectors. *Journal of Modern Optics*, 34(6-7):793, 1987.

[16] Jan Harms, Yanbei Chen, Simon Chelkowski, Alexander Franzen, Henning Vahlbruch, Karsten Danzmann, and Roman Schnabel. Squeezed-input, optical-spring, signal-recycled gravitational-wave detectors. *Physical Review D*, 68(4):042001, 2003.

[17] Hartmut Grote, K Danzmann, K L Dooley, R Schnabel, J Slutsky, and H Vahlbruch. First long-term application of squeezed states of light in a gravitational-wave observatory. *Physical Review Letters*, 110(18):181101, 2013.

[18] Rafał Demkowicz-Dobrzański, Konrad Banaszek, and Roman Schnabel. Fundamental quantum interferometry bound for the squeezed-light-enhanced gravitational wave detector geo 600. *Physical Review A*, 88(4):041802, 2013.

[19] S Dwyer, L Barsotti, SSY Chua, M Evans, M Facrouvich, D Gustafson, T Isogai, K Kawabe, A Khailovski, P K Lam, et al. Squeezed quadrature fluctuations in a gravitational wave detector using squeezed light. *Optics express*, 21(16):19047, 2013.

[20] Junaid Aasi, J Abadie, B P Abbott, Richard Abbott, T D Abbott, M R Abernathy, Carl Adams, Thomas Adams, Paolo Addesso, R X Adhikari, et al. Enhanced sensitivity of the ligo gravitational wave detector by using squeezed states of light. *Nature Photonics*, 7(8):613, 2013.

[21] Benjamin P Abbott, R Abbott, T D Abbott, M R Abernathy, F Acernese, K Ackley, C Adams, T Adams, P Addesso, R X Adhikari, et al. Gw150914: First results from the search for binary black hole coalescence with advanced ligo. *Physical Review D*, 93(12):122003, 2016.

[22] L P Grishchuk and Yu V Sidorov. Squeezed quantum states of relic gravitons and primordial density fluctuations. *Physical Review D*, 42(10):3413, 1990.

[23] L P Grishchuk. Quantum effects in cosmology. *Classical and Quantum Gravity*, 10(12):2449, 1993.

[24] Andreas Albrecht, Pedro Ferreira, Michael Joyce, and Tomislav Prokopec. Inflation and squeezed quantum states. *Physical Review D*, 50(8):4807, 1994.

[25] Bei Lok Hu, G W Kang, and Andrew Matacz. Squeezed vacua and the quantum statistics of cosmological particle creation. *International Journal of Modern Physics A*, 9(07):991, 1994.

[26] Martin B Einhorn and Finn Larsen. Squeezed states in the de sitter vacuum. *Physical Review D*, 68(6):064002, 2003.

[27] Claus Kiefer, Ingo Lohmar, David Polarski, and Alexei A Starobinsky. Pointer states for primordial fluctuations in inflationary cosmology. *Classical and Quantum Gravity*, 24(7):1699, 2007.

[28] Henning Vahlbruch, Simon Chelkowski, Karsten Danzmann, and Roman Schnabel. Quantum engineering of squeezed states for quantum communication and metrology. *New Journal of Physics*, 9(10):371, 2007.

[29] Vittorio Giovannetti, Seth Lloyd, and Lorenzo Maccone. Advances in quantum metrology. *Nature photonics*, 5(4):222, 2011.

[30] Radan Slavík, Francesca Parmigiani, Joseph Kakande, Carl Lundström, Martin Sjödin, Peter A Andrekson, Ruwan Weerasuriya, Stylianos Sygletos, Andrew D Ellis, Lars Grüner-Nielsen, et al. All-optical phase and amplitude regenerator for next-generation telecommunications systems. *Nature Photonics*, 4(10):690, 2010.

[31] V V Dodonov and A V Dodonov. Quantum harmonic oscillator and nonstationary casimir effect. *Journal of Russian Laser Research*, 26(6):445, 2005.

[32] J Robert Johansson, Göran Johansson, CM Wilson, and Franco Nori. Dynamical casimir effect in a superconducting coplanar waveguide. *Physical Review Letters*, 103(14):147003, 2009.

[33] J R Johansson, Göran Johansson, C M Wilson, and Franco Nori. Dynamical casimir effect in superconducting microwave circuits. *Physical Review A*, 82(5):052509, 2010.

[34] V V Dodonov. Current status of the dynamical casimir effect. *Physica Scripta*, 82(3):038105, 2010.

[35] Christopher M Wilson, Göran Johansson, Arsalan Pourkabirian, Michael Simoen, J Robert Johansson, Tim Duty, Franco Nori, and Per Delsing. Observation of the dynamical casimir effect in a superconducting circuit. *Nature*, 479(7373):376, 2011.

[36] Toshiyuki Fujii, Shigemasa Matsuo, Noriyuki Hatakenaka, Susumu Kurihara, and Anton Zeilinger. Quantum circuit analog of the dynamical casimir effect. *Physical Review B*, 84(17):174521, 2011.

[37] Pasi Lähteenmäki, GS Paraoanu, Juha Hassel, and Pertti J Hakonen. Dynamical casimir effect in a josephson metamaterial. *Proceedings of the National Academy of Sciences*, 110(11):4234, 2013.

[38] S Felicetti, M Sanz, L Lamata, G Romero, Göran Johansson, Per Delsing, and E Solano. Dynamical casimir effect entangles artificial atoms. *Physical Review Letters*, 113(9):093602, 2014.

[39] Masahiro Kitagawa and Masahito Ueda. Squeezed spin states. *Physical Review A*, 47(6):5138, 1993.

[40] Ian D Leroux, Monika H Schleier-Smith, and Vladan Vuletić. Implementation of cavity squeezing of a collective atomic spin. *Physical Review Letters*, 104(7):073602, 2010.

[41] Onur Hosten, Nils J Engelsen, Rajiv Krishnakumar, and Mark A Kasevich. Measurement noise 100 times lower than the quantum-projection limit using entangled atoms. *Nature*, 529(7587):505, 2016.

[42] Chin-wen Chou, D B Hume, J C J Koelemeij, David J Wineland, and T Rosenband. Frequency comparison of two high-accuracy al+ optical clocks. *Physical Review Letters*, 104(7):070802, 2010.

[43] John R Klauder and Bo-Sture Skagerstam. *Coherent states: applications in physics and mathematical physics*. World scientific, 1985.

[44] K Wodkiewicz and J H Eberly. Coherent states, squeezed fluctuations, and the su (2) am su (1, 1) groups in quantum-optics applications. *JOSA B*, 2(3):458, 1985.

[45] Jean-Pierre Gazeau. *Coherent states in quantum physics*. Wiley, 2009.

[46] Kôdi Husimi. Miscellanea in elementary quantum mechanics, ii. *Progress of Theoretical Physics*, 9(4):381, 1953.

[47] R Graham. Squeezing and frequency changes in harmonic oscillations. *Journal of Modern Optics*, 34(6-7):873, 1987.

[48] H Ralph Lewis Jr and W B Riesenfeld. An exact quantum theory of the time-dependent harmonic oscillator and of a charged particle in a time-dependent electromagnetic field. *Journal of mathematical physics*, 10(8):1458, 1969.

[49] V S Popov and A M Perelomov. Parametric excitation of a quantum oscillator. *Soviet Physics JETP*, 29(4):738, 1969.

[50] I A Malkin and V I Man'ko. Coherent states and excitation of n-dimensional nonstationary forced oscillator. Technical report, CM-P00062575, 1970.

[51] I A Malkin, V I Man'ko, and D A Trifonov. Coherent states and transition probabilities in a time-dependent electromagnetic field. *Physical Review D*, 2(8):1371, 1970.

[52] J Janszky and Y Y Yushin. Squeezing via frequency jump. *Optics communications*, 59(2):151, 1986.

[53] Xin Ma and William Rhodes. Squeezing in harmonic oscillators with time-dependent frequencies. *Physical Review A*, 39(4):1941, 1989.

[54] CF Lo. How does a squeezed state of a general driven time-dependent oscillator evolve? *Physica Scripta*, 42(4):389, 1990.

[55] C F Lo. Generating displaced and squeezed number states by a general driven time-dependent oscillator. *Physical Review A*, 43(1):404, 1991.

[56] G S Agarwal and S Arun Kumar. Exact quantum-statistical dynamics of an oscillator with time-dependent frequency and generation of nonclassical states. *Physical Review Letters*, 67(26):3665, 1991.

[57] J Janszky and P Adam. Strong squeezing by repeated frequency jumps. *Physical Review A*, 46(9):6091, 1992.

[58] T Kiss, P Adam, and J Janszky. Time-evolution of a harmonic oscillator: jumps between two frequencies. *Physics Letters A*, 192(5-6):311, 1994.

[59] T Kiss, J Janszky, and P Adam. Time evolution of harmonic oscillators with time-dependent parameters: A step-function approximation. *Physical Review A*, 49(6):4935, 1994.

[60] Héctor Moya-Cessa and Manuel Fernández Guasti. Coherent states for the time dependent harmonic oscillator: the step function. *Physics Letters A*, 311(1):1, 2003.

[61] D M Tibaduiza, L Pires, D Szilard, C A D Zarro, C Farina, and A L C Rego. A time-dependent harmonic oscillator with two frequency jumps: an exact algebraic solution. *Brazilian Journal of Physics*, 50(5):634, 2020.

[62] D M Tibaduiza, L Pires, A L C Rego, D Szilard, C Zarro, and C Farina. Efficient algebraic solution for a time-dependent quantum harmonic oscillator. *Physica Scripta*, 95(10):105102, 2020.

[63] D. Martínez-Tibaduiza, A.H. Aragão, C. Farina, and C.A.D. Zarro. New BCH-like relations of the  $su(1,1)$ ,  $su(2)$  and  $so(2,1)$  lie algebras. *Physics Letters A*, 384(36):126937, 2020.

[64] Stephen Barnett and Paul M Radmore. *Methods in theoretical quantum optics*, volume 15. Oxford University Press, 2002.

[65] M. Born and V. Fock. Beweis des adiabatensatzes. *Zeitschrift für Physik*, 51(3-4):165–180, mar 1928.

[66] I Averbukh, B Sherman, and G Kurizki. Enhanced squeezing by periodic frequency modulation under parametric instability conditions. *Physical Review A*, 50(6):5301, 1994.

[67] Shigemasa Matsuo, Toshiyuki Fujii, and Noriyuki Hatakenaka. Nonadiabatic squeezed-photon generation by a fourier-modified janszky–adam scheme. *Physica B: Condensed Matter*, 468:57, 2015.

[68] Xi Chen, A Ruschhaupt, Sebastian Schmidt, Adolfo del Campo, David Guéry-Odelin, and J Gonzalo Muga. Fast optimal frictionless atom cooling in harmonic traps: Shortcut to adiabaticity. *Physical Review Letters*, 104(6):063002, 2010.

[69] A Del Campo. Frictionless quantum quenches in ultracold gases: A quantum-dynamical microscope. *Physical Review A*, 84(3):031606, 2011.

[70] David Guéry-Odelin, Andreas Ruschhaupt, Anthony Kiely, Erik Torrontegui, Sofia Martínez-Garaot, and Juan Gonzalo Muga. Shortcuts to adiabaticity: Concepts, methods, and applications. *Reviews of Modern Physics*, 91(4):045001, 2019.

[71] Siegfried Grossmann and Martin Holthaus. On bose-einstein condensation in harmonic traps. *Physics Letters A*, 208(3):188, 1995.

[72] Fabienne Schneiter, Sofia Qvarfort, Alessio Serafini, André Xuereb, Daniel Braun, Dennis Rätzel, and David Edward Bruschi. Optimal estimation with quantum optomechanical systems in the nonlinear regime. *Physical Review A*, 101(3):033834, 2020.

[73] Sofia Qvarfort, Alessio Serafini, André Xuereb, Daniel Braun, Dennis Rätzel, and David Edward Bruschi. Time-evolution of nonlinear optomechanical systems: Interplay of mechanical squeezing and non-gaussianity. *Journal of Physics A: Mathematical and Theoretical*, 53(7):075304, 2020.

[74] Amy H. Skelt and Irene D'Amico. Characterizing adiabaticity in quantum many-body systems at finite temperature. *Advanced Quantum Technologies*, 3(7):1900139, 2020.

[75] Alejandro R Urzúa, Irán Ramos-Prieto, Manuel Fernández-Guasti, and Héctor M Moya-Cessa. Solution to the time-dependent coupled harmonic oscillators hamiltonian with arbitrary interactions. *Quantum Reports*, 1(1):82–90, 2019.

[76] Alejandro R Urzúa, Irán Ramos-Prieto, Francisco Soto-Eguibar, Víctor Arrizón, and Héctor M Moya-Cessa. Light propagation in inhomogeneous media, coupled quantum harmonic oscillators and phase transitions. *Scientific Reports*, 9(1):1, 2019.